Structure *14*, 345–355, February 2006 ©2006 Elsevier Ltd All rights reserved DOI 10.1016/j.str.2005.11.013

Structure and Specific RNA Binding of ADAR2 Double-Stranded RNA Binding Motifs

Richard Stefl,[1,3] Ming Xu,[2,3] Lenka Skrisovska,[1] Ronald B. Emeson,[2] and Frédéric H.-T. Allain[1,*]
[1]Institute of Molecular Biology and Biophysics
ETH Zürich
8093 Zürich
Switzerland
[2]Department of Pharmacology
Vanderbilt University
Nashville, Tennessee 37232

Summary

Adenosine deaminases that act on RNA (ADARs) site-selectively modify adenosines to inosines within RNA transcripts, thereby recoding genomic information. How ADARs select specific adenosine moieties for deamination is poorly understood. Here, we report NMR structures of the two double-stranded RNA binding motifs (dsRBMs) of rat ADAR2 and an NMR chemical shift perturbation study of the interaction of the two dsRBMs with a 71 nucleotide RNA encoding the R/G site of the GluR-B. We have identified the protein and the RNA surfaces involved in complex formation, allowing us to present an NMR-based model of the complex. We have found that dsRBM1 recognizes a conserved pentaloop, whereas dsRBM2 recognizes two bulged bases adjacent to the editing site, demonstrating RNA structure-dependent recognition by the ADAR2 dsRBMs. In vitro mutagenesis studies with both the protein and the RNA further support our structural findings.

Introduction

Adenosine deaminases that act on RNA (ADARs) convert adenosine to inosine (A-to-I) by hydrolytic deamination in cellular and viral RNA transcripts containing either perfect or imperfect regions of double-stranded RNA (dsRNA) (Bass, 2002; Emeson and Singh, 2000; Gerber and Keller, 2001; Keegan et al., 2001). To date, two functional enzymes (ADAR1 and ADAR2), and one inactive enzyme (ADAR3), have been characterized in mammals. A-to-I modification is nonspecific within perfect dsRNA substrates, deaminating up to 50% of the adenosine residues (Bass, 2002; Emeson and Singh, 2000). The nonspecific reaction occurs as long as the double-stranded architecture of the RNA substrate is maintained, since ADARs unwind dsRNA by changing A-U base pairs to I-U mismatches (Bass and Weintraub, 1988). The majority of nonselective editing occurs in untranslated regions (UTRs) and introns, where large regular duplexes are formed (Levanon et al., 2004; Morse et al., 2002; Morse and Bass, 1999; Rueter et al., 1999). Such modifications can modulate gene silencing triggered by intramolecular structures in mRNA (Tonkin and Bass, 2003), nuclear retention of RNA transcripts (Zhang and Carmichael, 2001), or antiviral responses by extensive modification of viral transcripts (Wong et al., 1991).

A-to-I editing can also be highly specific within imperfect dsRNA regions containing bulges, loops, and mismatches, and it can modify a single or limited set of adenosine residues (Bass, 2002; Emeson and Singh, 2000). Selective editing within pre-mRNAs has been shown to affect the primary amino acid sequence of the resultant protein product to produce multiple protein isoforms from a single gene. For example, ADARs have been shown to produce functionally important isoforms of numerous proteins involved in synaptic neurotransmission, including ligand and voltage-gated ion channels and G protein-coupled receptors (Bhalla et al., 2004; Burns et al., 1997; Egebjerg and Heinemann, 1993; Hoopengardner et al., 2003; Kohler et al., 1993; Lomeli et al., 1994; Sommer et al., 1991). The pre-mRNA encoding the B subunit of the α-amino-3-hydroxy-5-methyl-4-isoxazole propionic acid (AMPA) subtype of glutamate receptor (GluR-B) has been studied extensively and is edited at multiple sites (Seeburg et al., 1998). One of these locations is the R/G site, where a genomically encoded AGA is modified to IGA, resulting in an arginine-to-glycine change (the ribosome interprets I as G due to its similar base-pairing properties). This change affects the biophysical properties of the ion channel allowing the edited isoform to recover faster from desensitization (Lomeli et al., 1994). The R/G site of the GluR-B pre-mRNA is often used as a model system for A-to-I editing studies, as it forms a small and well-conserved ~70 nucleotide (nt) stem-loop containing three mismatches (Aruscavage and Bass, 2000); this structure is referred to as the R/G stem-loop.

Like many RNA binding proteins, ADARs display a modular domain organization. ADARs contain from one to three tandem copies of double-stranded RNA binding motif (dsRBMs) in their N-terminal region and an adenosine deaminase domain, the structure of which has recently been determined, in its C-terminal portion (Macbeth et al., 2005). The dsRBMs of ADARs may play an important role in modulating the editing selectivity of ADARs (Carlson et al., 2003; Doyle and Jantsch, 2002; Stephens et al., 2004). The dsRBM is a 70–75 amino acid domain found in many eukaryotic proteins with diverse functions (Fierro-Monti and Mathews, 2000). The structures of several dsRBMs have been determined (Bycroft et al., 1995; Kharrat et al., 1995; Nanduri et al., 1998) and reveal a highly conserved αββββα protein topology in which the two α helices are packed along a face of a three-stranded antiparallel β sheet. Furthermore, structures of the dsRBMs from *Xenopus laevis* RNA binding protein A (Xlrbpa2) (Ryter and Schultz, 1998), *Drosophila* Staufen protein (Ramos et al., 2000), and *Aquifex aeolicus* RNase III (Blaszczyk et al., 2004), in complex with nonnatural synthetic dsRNA substrates, have been determined; the dsRBM of Rnt1p (an RNase III homolog from budding yeast) has been determined in complex with its natural RNA substrate (dsRNA capped by an AGAA tetraloop) (Wu et al., 2004). These

*Correspondence: allain@mol.biol.ethz.ch
[3]These authors contributed equally to this work.

structures revealed not only how dsRBMs can bind any dsRNA, regardless of base composition, but also how structure-specific recognition of RNA hairpins is achieved (reviewed in Stefl et al., 2005a).

While the enzymatic activity of ADARs and their biological role(s) have extensively been studied (Bass, 2002; Emeson and Singh, 2000), the determinants that control site-selective RNA modification are poorly understood. Here, we report the solution structure of the two dsRBMs of ADAR2 and their interactions with the conserved 71 nt RNA stem-loop containing the GluR-B R/G site (R/G stem-loop). We show that each dsRBM binds a different structural element of the R/G stem-loop, and that dsRBM1 and dsRBM2 recognize a stem capped by a pentaloop and a stem containing two A-C mismatches, respectively. Our structural study demonstrates that the dsRBMs of ADAR2 have the ability to distinguish between specific structural features of RNA, suggesting their importance for editing site selectivity.

Results

ADAR2 dsRBMs Are Independent Domains

We investigated the N-terminal region of rat ADAR2 (74–301) that includes the dsRBM1 (74–147), the interdomain linker (148–230), and dsRBM2 (231–301) by using NMR spectroscopy (Figure 1A). This protein construct was aminoterminally fused with noncleavable solubility-enhancement tag GB1 (Zhou et al., 2001) to improve its expression and solubility (Stefl et al., 2005b). ^{1}H, ^{13}C, and ^{15}N resonance assignments of GB1-dsRBM12 and of the two isolated dsRBMs were obtained as previously described (Stefl et al., 2005b). As the spectral quality of the 32 kDa GB1-dsRBM12 suffered from an increased transverse relaxation, we used hydrogen-to-deuteron substitutions at various levels to improve the relaxation properties of the protein (Stefl et al., 2005b). The comparison between the [^{1}H,^{15}N]-TROSY spectrum of a deuterated GB1-dsRBM12 and the [^{1}H,^{15}N]-HSQC spectra of both isolated dsRBM1 and dsRBM2 (Figure S1; see the Supplemental Data available with this article online) shows that the dsRBM resonances are identical in both contexts, except for a few N- and C-terminal residues. In addition, this comparison indicates that the interdomain linker is flexible, as the chemical shifts of the linker residues have random coil values (Stefl et al., 2005b). To determine whether the chemical shift differences of the terminal residues of the isolated dsRBMs and GB1-dsRBM12 are due to involvement in interdomain contacts or due to different flanking residues at the termini, we carefully analyzed and compared the [^{1}H,^{13}C]-HSQC, ^{15}N- and ^{13}C-separated NOESY data of a 50%-deuterated GB1-dsRBM12 with data from the corresponding experiments of the isolated dsRBM1 and dsRBM2. However, no interdomain NOEs could be observed. Furthermore, when the isolated dsRBM1 and dsRBM2 were mixed in *trans*, the [^{1}H,^{15}N]-HSQC spectrum showed no change of chemical shifts compared to the two [^{1}H,^{15}N]-HSQC spectra of the isolated domains (data not shown). These results indicate that the ADAR2 dsRBMs are independent domains separated by a flexible linker, similar to the two dsRBMs of PKR (Nanduri et al., 1998). Thus, we used separate dsRBM1 and dsRBM2 constructs to determine their structures by NMR.

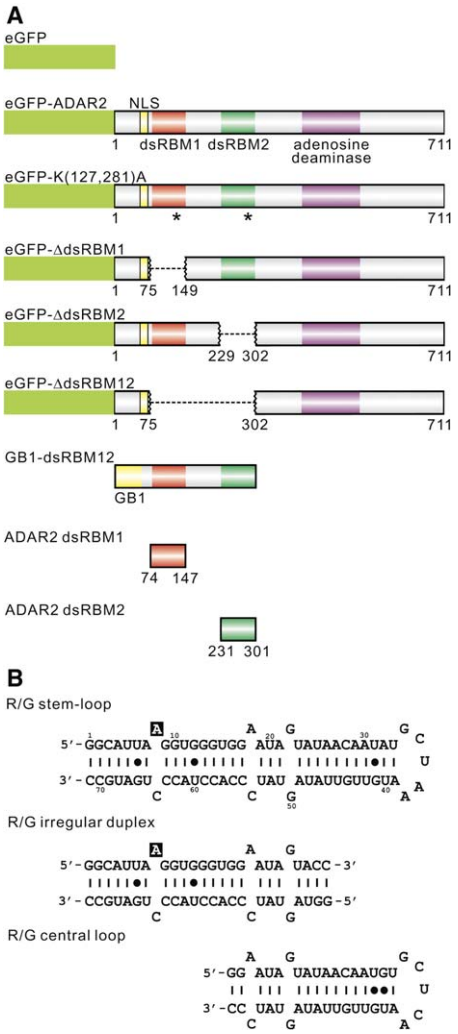

Figure 1. Protein and RNA Constructs Used for NMR and Functional Analysis

(A) A schematic diagram indicating the structure of eGFP, wild-type eGFP-ADAR2, eGFP-K(127,281)A double mutant (the position of point mutations are labeled by an asterisk), mutant fusion proteins (showing deletion of dsRBM1, dsRBM2, and dsRBM12), as well as GB1-dsRBM12, ADAR2 dsRBM1, and ADAR2 dsRBM2 is presented. The coordinates of each deletion are indicated, relative to the start codon. NLS, nuclear localization signal. GB1, immunoglobulin binding domain B1 of streptococcal protein G, is a noncleavable solubility-enhancement tag (Zhou et al., 2001).

(B) R/G stem-loop, a 71 nt stem-loop that includes the 67 nt of the human GluR-B mRNA stem-loop and is closed by two GC base pairs to improve the yield from in vitro transcription. R/G irregular duplex, a 52 nucleotide duplex embedding the R/G editing site of the rat R/G stem-loop, closed by two GC base pairs at both ends of the duplex. R/G central loop, a 41 nt stem-loop, represents the central part of the rat GluR-B R/G mRNA. Note that rat and human RNA sequences of the GluR-B mRNA R/G stem-loop are identical, except for two nucleotides in the central loop part, G32A and C37A, which do not affect the fold of this region (R.S. and F.H.-T.A., unpublished data). Furthermore, rat and human ADAR2 dsRBM1, a domain interacting with the central part of GluR-B R/G mRNA, are identical within the structured domain.

ADAR2 dsRBM Structures Are Not Identical

The structures of dsRBM1 and dsRBM2 were determined by using 1754 and 1459 conformationally restrictive NOE distance restraints, respectively, derived from

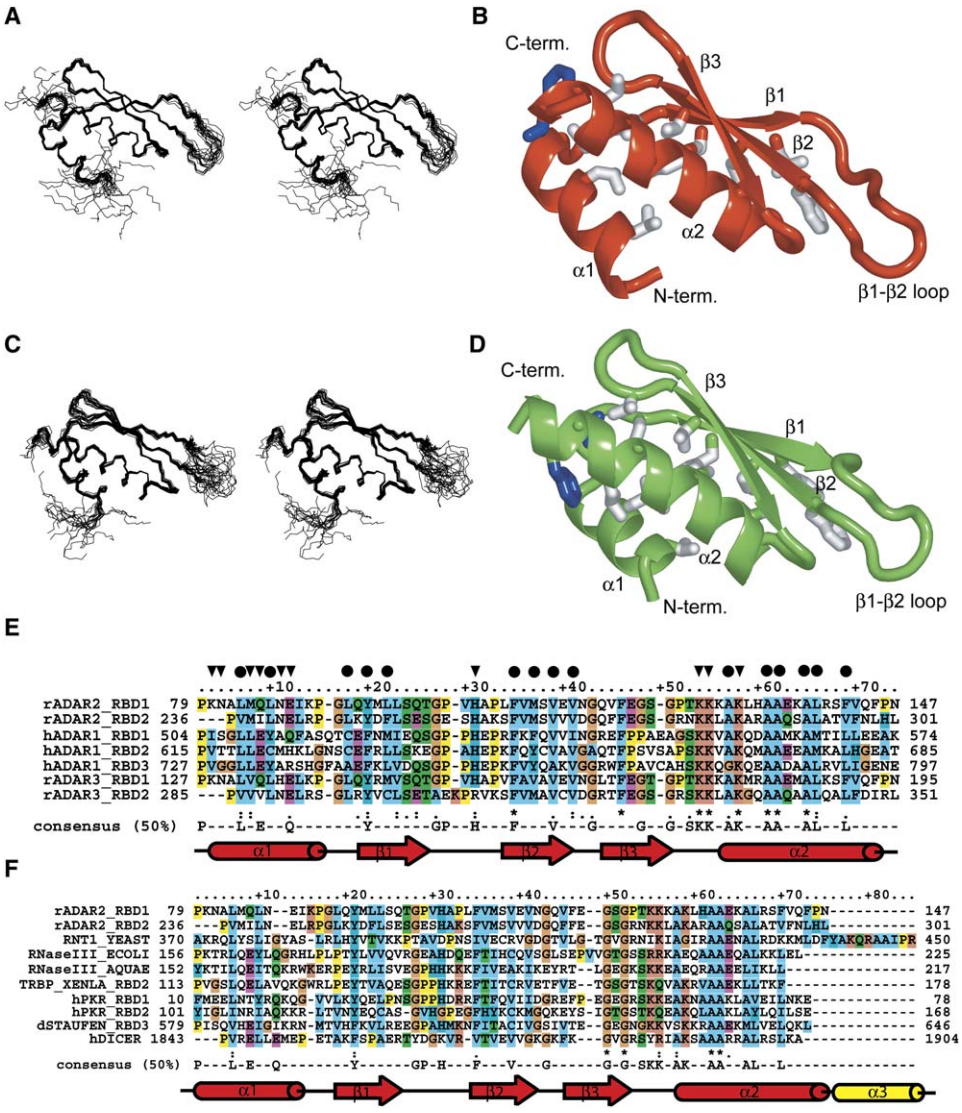

Figure 2. ADAR2 dsRBMs' Protein Structure

(A–D) NMR ensemble of (A) dsRBM1 and (C) dsRBM2; 20 lowest-energy structures. Ribbon representation of (B) dsRBM1 (in red) and (D) dsRBM2 (in green) with conserved hydrophobic core residues (sticks, in white).

(E) Sequence alignment of various dsRBMs of ADARs. Two dsRBMs of rat ADAR2, three dsRBMs of human ADAR1, and two dsRBMs of rat ADAR3. The consensus sequence (>50%) of dsRBMs (Fierro-Monti and Mathews, 2000) and a schematic of secondary structure elements of dsRBM are indicated below. The residues of the conserved hydrophobic core and the RNA binding surface are indicated by black dots and triangles, respectively.

(F) Sequence alignment of various dsRBMs. Two dsRBMs of rat ADAR2, dsRBM of Rnt1p (*S. cerevisiae*), dsRBM of RNase III (*E. coli*), dsRBM of RNase III (*A. aeolicus*), second dsRBM of Xlrbpa (*X. laevis*), dsRBM1 and dsRBM2 of PKR (*H. sapiens*), dsRBM3 of Staufen (*D. melanogaster*), and dsRBM of DICER (*H. sapiens*).

2D homonuclear and 3D ^{13}C- and ^{15}N-edited NOESYs. The resulting structures are represented by an ensemble of 20 conformers for both dsRBM1 and dsRBM2 (Figure 2). The ensembles have root mean square deviations of 0.45 ± 0.10 and 0.52 ± 0.12 Å over the backbone in the structured regions for dsRBM1 and dsRBM2, respectively. A full summary of structural statistics is given in Table 1. Both the ADAR2 dsRBM1 and dsRBM2 structures adopt the same fold as all other members of the dsRBM family, with an $\alpha\beta\beta\beta\alpha$ topology in which the two α helices are packed along a face of a three-stranded antiparallel β sheet (Figure 2). A central hydrophobic core composed of the residues shown in Figure 2 (Figures 2B and 2D for structural arrangement, and Figure 2E for sequence alignment) stabilizes the fold of the domain. Although the two dsRBMs of ADAR2 have 50% amino acid identity, the two structures differ slightly in the orientation of α helix 1 relative to the other secondary structure elements (Figure 2). This altered orientation is a result of a protein sequence difference in two amino acids at the C terminus of α helix 2, where Phe142 and Val143 in dsRBM1 are replaced by Val296 and Phe297 in dsRBM2. Phe297, compared to Val143, is bulkier, leading to a different interaction between the two α

Table 1. NMR Experimental Constraints and Structure Statistics

	dsRBM1	dsRBM2
Distance constraints		
NOE upper distance limits	1754	1459
Structure statistics[a]		
NOE violations		
Number (>0.3 Å)	0.85 ± 1.13	2.00 ± 1.34
Maximum violations (Å)	0.33 ± 0.13	0.39 ± 0.04
Rmsd from the mean coordinates (Å)[a]		
Only secondary structure elements (residues 6–25, 36–68 for dsRBM1, and 6–22, 33–65 for dsRBM2)		
Backbone	0.45 ± 0.10	0.52 ± 0.12
Heavy atoms	1.07 ± 0.16	1.29 ± 0.14
Entire domain		
Backbone	0.80 ± 0.25	1.34 ± 0.36
Heavy atoms	1.28 ± 0.23	2.13 ± 0.35
Rmsd from ideal geometry[a]		
Bonds lengths (Å)	0.0099 ± 0.0002	0.0106 ± 0.0002
Bond angles (°)	2.5127 ± 0.0309	2.5448 ± 0.0456
Ramachandran analysis (%)[b]		
Most favored region	86	82.4
Allowed region	13.1	16.2
Disallowed region	0.9	1.4

[a] The statistics (average ± SDs) calculated for the bundle of the 20 best-energy conformers.
[b] As determined by PROCHECK (Laskowski et al., 1996).

helices (Figure 2D, in blue). We found another difference between the two dsRBMs in the conformation of the β1-β2 loop. The β1-β2 loop of dsRBM1 is well defined, whereas the β1-β2 loop of dsRBM2 is conformationally heterogeneous (Figures 2A and 2C). In dsRBM2, several amide resonances of this loop are not observable in the spectra, probably due to a conformational exchange, whereas all of the amide proton resonances of the β1-β2 loop of dsRBM1 were observed and involved in many NOE correlations. These observations suggest that the β1-β2 loop of dsRBM1 is more rigid than the β1-β2 loop of dsRBM2, which is probably due to the presence of two prolines in dsRBM1 that are not found in dsRBM2 (Figure 2E). Flexible β1-β2 loops were also observed in other dsRBM structures (Leulliot et al., 2004; Ramos et al., 2000). Altogether, the longer α helix 1 and the conformationally preorganized β1-β2 loop of dsRBM1 might be important factors for ADAR2 RNA recognition.

Mapping of the RNA Binding Surface on the ADAR2 dsRBMs

To investigate how ADAR2 dsRBMs bind RNA, we performed an NMR chemical shift perturbation study with a 71 nt R/G stem-loop RNA (Figure 1B). This RNA is a 33 bp helix containing three mismatches (two A-C and one G-G) that is capped by a structured pentaloop (Stefl and Allain, 2005). A8 of this RNA can be specifically edited (up to 74%) by ADAR2 in vitro, but if the mismatches are replaced by Watson-Crick base pairs, the editing efficiency is reduced substantially (Kallman et al., 2003; Ohman et al., 2000).

First, we studied the interaction between GB1-dsRBM12 and the 71 nt R/G stem-loop (Figure 1). Upon RNA titration up to an equimolar ratio, the protein resonances showed significant chemical shift changes when followed by [^{1}H,^{15}N]-TROSY spectra; however, we could not assign the protein resonances of this 55 kDa GB1-dsRBM12-R/G stem-loop complex due to severe line broadening (Figure S2). As the dsRBMs are independent in the free form, we presumed that they could have different binding sites on the R/G stem-loop. Therefore, we used two truncations of the R/G stem-loop, a 52 nt R/G irregular duplex and a 41 nt R/G central loop (Figure 1). We prepared four complexes (the two truncated RNAs bound to each dsRBM) and measured a [^{1}H,^{15}N]-HSQC spectrum for each. The chemical shifts in the [^{1}H,^{15}N]-HSQC spectra of dsRBM1 bound to the R/G central loop and of dsRBM2 bound to the R/G irregular duplex complexes were virtually identical to the ones in the [^{1}H,^{15}N]-TROSY spectrum of the full-length complex (Figure S2). These observations indicate that the dsRBMs are bound in the same manner in these two subcomplexes and in the full-length complex (GB1-dsRBM12 bound to the R/G stem-loop). The two dsRBMs of ADAR2 bind two distinct locations on the R/G stem-loop; dsRBM1 binds close to the pentaloop, and dsRBM2 binds close to the editing site. The NMR data of the reciprocal complexes (dsRBM2 bound to the R/G central loop and dsRBM1 bound to the R/G irregular duplex complexes) indicated that such subcomplexes are formed; however, their chemical shift values do not resemble the ones observed in the full-length complex. Furthermore, the spectra of these two subcomplexes showed severe line broadening, probably resulting from exchange between multiple protein-RNA complexes of similar affinities. These observations indicated that the binding of both dsRBMs is specific.

To gain more detailed insights into the interactions between the ADAR2 dsRBMs and the R/G stem-loop, the backbone amide resonances of the dsRBM1 and dsRBM2 in the subcomplexes were assigned. In both dsRBMs, the largest chemical shift changes between the free and the bound forms were observed for the backbone amides of α helix 1 and the β1-β2 loop (Figure 3). In addition, large chemical shift changes were observed for the β3-α2 loop and the N terminus of α helix 2 of dsRBM1, whereas no large chemical shift changes were observed for the dsRBM2 in these two regions. These results are surprising since these regions of dsRBM1 and dsRBM2 are similar in sequence with the presence of three conserved lysines (Figure 2E). Taken together, the patterns of chemical shift perturbations indicate that the protein-RNA interactions are different between dsRBM1 and dsRBM2, reflecting the structural differences already observed in the free dsRBMs structures. The RNA binding surfaces identified by chemical shift perturbations in both dsRBMs agree well with the positive electrostatic potential calculated by using a nonlinear Poisson-Boltzmann equation (Figures 3C and 3F). In particular, the stretch of lysines located in the β3-α2 loop and the N terminus of α helix 2 found in both dsRBMs (Figure 2E) create the region with the highest potential. The RNA binding surfaces of ADAR2 dsRBM1 and dsRBM2, although not identical, are similar to the ones observed in other dsRBMs-RNA complexes (Blaszczyk et al., 2004; Ramos et al., 2000; Ryter and Schultz, 1998; Wu et al., 2004).

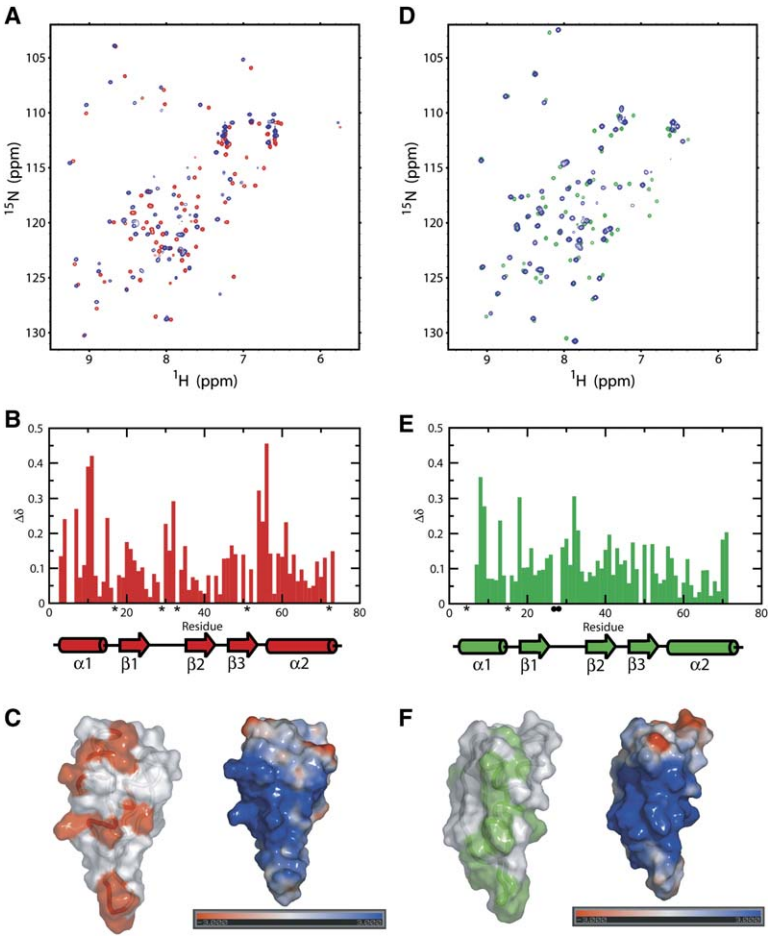

Figure 3. RNA Binding Surfaces of ADAR2 dsRBMs

(A–C) dsRBM1-R/G central loop. (A) Overlay of [^{1}H-^{15}N]-HSQC spectra of dsRBM1 (in red) and the dsRBM1-R/G central loop complex (in blue). (B) Chemical shift changes (Δδ) for dsRBM1 upon addition of the R/G central loop. The Δδ is calculated as $([\omega_{HN}\Delta\delta_{HN}]^2 + [\omega_N\Delta\delta_N]^2)^{1/2}$, where $\omega_{HN} = 1$ and $\omega_N = 0.154$ are weight factors of the nucleus (Mulder et al., 1999); asterisk, proline. (C) Δδ upon RNA binding mapped to the surface of the protein identifies the RNA binding surface of dsRBM1 (left; in red; $\Delta\delta \geq 0.15$ are displayed). The electrostatic surface of dsRBM1 (right).

(D–F) dsRBM2-R/G irregular duplex. (D) Overlay of [^{1}H-^{15}N]-HSQC spectra of dsRBM2 (in green) and the dsRBM2-R/G irregular duplex complex (in blue). (E) Δδ for dsRBM2 upon addition of R/G irregular duplex (asterisk, proline; closed, black circle, unassigned). (F) Δδ upon RNA binding mapped to the surface of the protein identifies the RNA binding surface of dsRBM2 (left; in green). The electrostatic surface of dsRBM2 (right).

Mapping of the Protein Binding Surface on the R/G Stem-Loop

To investigate the protein binding surface, the resonances of the 71 nt R/G stem-loop were assigned as described in the Supplemental Data. The NMR data showed the presence of a G22-G50 mismatch and two "open" A-C mismatches (A8-C64 and A18-C54). Based on these data, together with our NMR structure of the central pentaloop region of the human R/G stem-loop (Stefl and Allain, 2005), we built a structural model of the rat 71 nt R/G stem-loop (Figure 4D).

Upon protein binding to the 71 nt R/G stem-loop, the RNA imino proton resonances broaden continuously as a result of chemical exchange and increased molecular weight. However, no significant chemical shift changes and no new imino proton resonances were observed, indicating that no changes in the RNA secondary structure take place upon complex formation. In the two subcomplexes of dsRBM1 bound to the R/G central loop and dsRBM2 bound to the R/G irregular duplex, a precise analysis of the pyrimidine H5 and H6 chemical shift perturbations upon protein binding could be done with a series of 2D-[^{1}H,^{1}H]-TOCSY spectra (Figure 4). In the course of the protein titrations, the resonances moved from their initial positions, which correspond to the free form, in a stepwise directional manner until they reached their final positions, which correspond to the fully bound state (example shown in Figures 4A and 4B). These data indicate that, in both subcomplexes, the RNAs are in fast exchange between their free and bound forms relative to the NMR timescale. The binding of dsRBM1 to the R/G central loop induces a significant chemical shift perturbation of C37 and U40 (Figures 4A and 4B), and the binding of dsRBM2 to the R/G irregular duplex causes pyrimidine perturbations of C54, C55, C56, C63, C64, and U65; C54 and C64 experience the largest chemical shift changes (Figure 4C). These chemical shift changes strongly suggest that the above-mentioned RNA bases are interacting with the proteins or a significantly changed conformation (for C54 and C64) as they become stacked within the duplex upon protein binding. We find the latter explanation less likely, as the C54 and C64 H5 and H6 resonances are still in the chemical shift range of unpaired nucleotide and no new imino protons are observed upon protein binding. Figure 4D displays the pyrimidine residues with the largest chemical shift perturbations on the 3D NMR model of the R/G stem-loop.

The study of the reversed subcomplexes, dsRBM1 bound the R/G irregular duplex and dsRBM2 bound to the R/G central loop, showed that dsRBM1 contacts C54 and C64 on the R/G irregular duplex as well, whereas dsRBM2 only binds the stem (where one A-C mismatch, C64, is present), not the pentaloop of the central R/G stem-loop (data not shown).

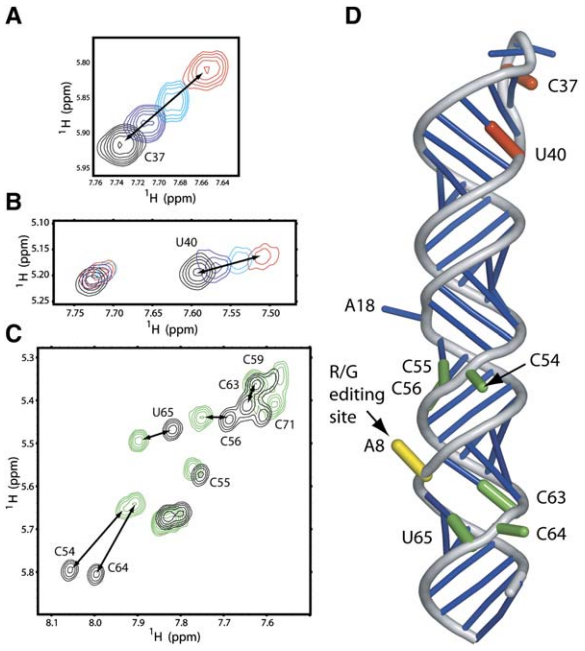

Figure 4. Protein Binding Surfaces of the R/G Stem-Loop

(A and B) dsRBM1-R/G central loop. Overlay of series 2D [^{1}H-^{1}H]-TOCSY spectra (focused on a portion with H5-H6 resonances of C37, U25, and U40) of the titration experiment in which the dsRBM1 was successively added in the following molar ratios: 0:1 (free RNA) (in black), 1/3:1 (in blue), 2/3:1 (in cyan), and 1:1 (fully bound RNA) (in red).

(C) dsRBM2-R/G irregular duplex. Overlay of 2D [^{1}H-^{1}H]-TOCSY spectra of free (in black) and fully bound RNA (in green), focused on a portion with strongly shifted H5-H6 resonances.

(D) Chemical shift changes upon protein binding mapped to an NMR model of the R/G stem-loop. The nucleotides in red and green are affected upon dsRBM1 and dsRBM2 binding, respectively.

ADAR2 dsRBMs Do Not Dimerize on the R/G Stem-Loop

It has been reported that ADAR activation involves RNA-dependent dimerization (Cho et al., 2003; Gallo et al., 2003; Jaikaran et al., 2002). To test whether more than two ADAR2 dsRBMs could bind the 71 nt R/G stem-loop, we performed light-scattering experiments. We incubated GB1-dsRBM12 with the R/G stem-loop at protein:RNA stochiometric ratios of 0.5:1, 1:1, 2:1, and 4:1, and we analyzed them by using gel filtration coupled with in-line laser light scattering. At the ratio of 1:1, a single peak with the expected size (MW ~55 kDa) of the bimolecular complex appeared. In all other ratios, peaks of either unbound RNA or protein, in addition to the peak of the bimolecular complex, appeared in the chromatogram. This indicates that only one molecule of GB1-dsRBM12 can be accommodated by the R/G stem-loop, and that the peptide sequence responsible for the dimerization is outside the RNA binding region of ADAR2 (74–301).

NMR Model of ADAR2 dsRBM12 in Complex with the R/G Stem-Loop

To understand the basic principles of this recognition, we constructed a model of ADAR2 dsRBMs in complex with the 71 nt R/G stem-loop based on our precise NMR identification of both the protein and RNA interaction surfaces and on the knowledge of the basic structural elements controlling dsRBMs-RNA recognition (Stefl et al., 2005a). We performed a docking search by using a methodology similar to the one implemented in HADDOCK (Dominguez et al., 2003). In docking calculations, we used the NMR ensembles of the dsRBM1 and dsRBM2 and multiple MD-generated conformations of the R/G stem-loop model as starting structures. We took advantage of the fact that there are no major changes in the backbone conformation of the dsRBMs upon RNA binding (Leulliot et al., 2004; Ramos et al., 2000; Wu et al., 2004), and that dsRBMs contact RNA via a well-conserved interaction scheme (Stefl et al., 2005a). Both facts provided the constraints that significantly reduced the degrees of freedom of the conformational docking search. Furthermore, the docking was guided by the information obtained from our NMR chemical shift perturbation studies that identified the protein and RNA interaction surfaces.

Figure 5A shows the resulting NMR model with the lowest energy of the ADAR2 dsRBM12-R/G stem-loop complex. In a similar manner to what was observed for the Rnt1p dsRBM-AGNN tetraloop-containing RNA complex (Wu et al., 2004), the dsRBM1 contacts the minor groove of the GCUCA pentaloop and the adjacent G-U mismatch of the central region of the R/G stem-loop. The dsRBM2 interacts with the bulged C54 and C64 opposite the editing site. Among the dsRBM-dsRNA complexes determined to date, the interaction of ADAR2 dsRBM2 is unique, since dsRBM2 appears to recognize two bulged cytosines. This is reminiscent of CCHH-type zinc fingers that are also able to recognize RNA bases that bulge out of the rigid structural architecture (Lu et al., 2003). dsRBMs are considered to be structure-specific rather than sequence-specific RNA binding proteins (Stefl et al., 2005a). Based on our NMR model of the complex, the dsRBMs of ADAR2 are not an exception, since dsRBM1 recognizes a stem-loop structure and dsRBM2 recognizes an RNA helix containing two A-C mismatches separated by ten base pairs.

Both ADAR2 dsRBMs Are Important for Efficient Editing of the R/G Site

To investigate whether both ADAR2 dsRBM-RNA interactions are important for ADAR2-mediated editing of the R/G site, either dsRBM1 or dsRBM2 was deleted from an eGFP-ADAR2 fusion protein (Figure 1A), which has been previously shown to have a comparable enzymatic activity to wild-type ADAR2 protein (Sansam et al., 2003). We took advantage of an in vitro editing system that used the R/G editing substrate and wild-type or mutant eGFP-ADAR2 proteins in HEK293 nuclear extracts. Preliminary time course analyses with wild-type eGFP-ADAR2 protein were used to define the linear range of the in vitro editing reaction (data not shown), and equivalent amounts of wild-type and mutant proteins, as determined by quantitative Western blotting, were incubated with an in vitro-transcribed R/G editing substrate (Dawson et al., 2004). Nuclear extracts from eGFP-transfected cells defined background editing levels for the in vitro system, while the wild-type eGFP-ADAR2 protein demonstrated robust editing of the R/G site (Figure 5E). Deletion of either dsRBM1 or dsRBM2 dramatically decreased the editing on R/G site by 3- to 10-fold, while

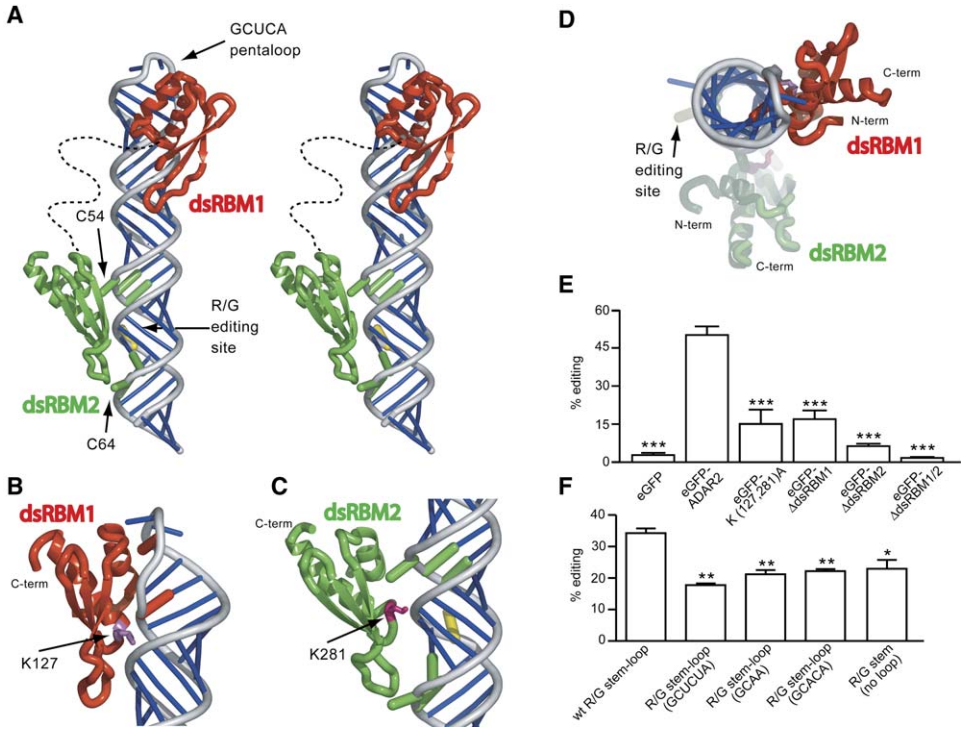

Figure 5. ADAR2-Mediated Editing of the R/G Site Requires Both dsRBMs

(A) Overall NMR model of ADAR2 dsRBM12 in complex with the R/G stem-loop (stereoview).

(B) dsRBM1 (in red) interacts with the central part of the R/G stem-loop; α helix 1 contacts the pentaloop and the adjacent G-U base pair.

(C) dsRBM2 interacts with bulged cytosines, opposite the editing site. K127 and K281, residues mutated to alanine in our functional studies are shown in magenta and pink, respectively.

(D) Overall NMR model (top view).

(E) Quantitative analysis of RNA editing for the R/G site from in vitro editing analyses with wild-type, eGFP-K(127,281)A, and mutant eGFP-ADAR2 fusion constructs lacking either dsRBM1 or dsRBM2 and both of them (mean ± SEM; n = 5); **p < 0.01; ***p < 0.001 compared to wild-type eGFP-ADAR2 (using the Student's t test).

(F) Various mutations introduced in the loop region of the R/G stem-loop and their role on editing efficiency at the R/G site. Mutations include: GCUCA pentaloop replaced by a GCUCUA hexaloop, by a GCAA tetraloop, and by a GCACA pentaloop. All of these mutations change the conformation of the loop. In addition, we used RNA in which the pentaloop of the R/G stem-loop is removed and in which the stem sequence is conserved ("R/G stem"). All mutants were assayed for editing activity at the R/G site in vitro by using wild-type eGFP-ADAR2 (mean ± SEM; n = 3); **p < 0.01; *p < 0.03 compared to wild-type eGFP-ADAR2 (using the Student's t test).

deletion of both dsRBMs (eGFP-ΔdsRBM12) completely eliminated A-to-I conversion at the R/G site (Figure 5E). In addition, simultaneous mutations of the two highly conserved K127 (dsRBM1) and K281 (dsRBM2) displayed significantly lower editing activity at the R/G site (Figure 5E), further confirming the importance of RNA binding of both domains for editing, as both side chains are predicted in our NMR model to interact with the sugar-phosphate backbone (Figures 5B and 5C).

Functional Importance of the R/G Stem-Loop Secondary Structure for Editing by ADAR2

Our NMR study shows that both dsRBM1 and dsRBM2 bind specific region of the R/G stem-loop; dsRBM1 binds near the pentaloop, and dsRBM2 binds the stem with two A-C mismatches in the neighborhood of the R/G editing site (Figure 5A). The functional importance of the A-C mismatches was previously shown, as their replacement by Watson-Crick base pairs decreases the editing from 74% to 41% (Ohman et al., 2000) and its selectivity for the R/G site from 80% to 30% (Kallman et al., 2003). To assess the functional importance of the pentaloop, we created several mutants in the loop region of the R/G stem-loop (Figure 5F), and we assayed them for editing activity at the R/G site in vitro. These mutants include a variation in the GCUCA pentaloop sequence (GCACA; a single mutation that changes the fold of the loop [Stefl and Allain, 2005]) and variations in the loop size (GCAA tetraloop and GCUCUA hexaloop). All of these mutants display lower editing efficiency at the R/G site compared to the wild-type (Figure 5F), indicating that the pentaloop sequence GCUCA and its specific structure are functional determinants of the editing at the R/G site. In addition, an R/G stem-loop mutant lacking the entire GCUCA pentaloop (R/G stem) also has lower editing activity at the R/G site (Figure 5F). Altogether, changes in the sequence or in the size of the pentaloop that lead to a different pentaloop topology result in lower editing efficiency at the R/G site, indicating the functional importance of the pentaloop structure (Stefl and Allain, 2005).

Discussion

Structure of ADAR2 dsRBMs: Comparison and Implications

In comparison to other dsRBMs, ADAR2 dsRBM1 and dsRBM2 differ from the canonical dsRBM fold like the

ones of Xlrbpa2 (Ryter and Schultz, 1998) and *Aquifex aeolicus* RNase III (Blaszczyk et al., 2004) (Figure S4A, in white). Interestingly, ADAR2 dsRBM1 resembles the dsRBM of Rnt1p (Figure S4B, in blue) (Leulliot et al., 2004); however, it lacks α helix 3, an additional element that imposes the conformation of the "recognition" α helix 1 in the dsRBM of Rnt1p. ADAR2 dsRBM2 appears to be unique among other members of the dsRBM family (Figure S4). This structural difference in the relative orientation of α helix 1 may be functionally important, as it is a key element that modulates the RNA binding specificity of dsRBMs (Ramos et al., 2000; Stefl et al., 2005a; Wu et al., 2004) (see below).

How Do ADAR2 dsRBMs Recognize the R/G Stem-Loop?

With dsRBM-containing proteins, questions regarding binding specificities have always been difficult to answer, as this abundant RNA binding domain is considered to bind any dsRNA in a non-sequence-specific manner. Structures of single dsRBMs in complex with dsRNA indeed revealed that dsRBMs are not sequence-specific RNA binders, but they raised the question of whether dsRBMs would rather recognize certain RNA structures, like stem-loops or irregular duplexes (Ramos et al., 2000; Stefl et al., 2005a; Wu et al., 2004). Our extensive binding study of ADAR2 dsRBMs with the GluR-B R/G stem-loop and our structural model further extends our understanding of how ADAR2 dsRBMs recognize their targets and, more generally, how dsRBMs recognize RNA.

dsRBMs are often present in multiple nonidentical copies in proteins. In studying the two dsRBMs of ADAR2, we provide one of the first structural studies on how two domains work together. Surprisingly, although both dsRBMs are essential for efficient RNA editing, they apparently bind the RNA independently, as the interdomain linker (147–231) that bridges the dsRBMs of ADAR2 is found to be unstructured in both the free and bound forms of the protein and does not appear to participate in the interaction with the R/G stem-loop. This contrasts with what was found for other RNA recognition motifs, in which the interdomain linkers play a critical role in RNA recognition (Allain et al., 2000; Deo et al., 1999; Handa et al., 1999). Another surprising result is that both dsRBMs are bound in a well-defined location on the R/G stem-loop (dsRBM1 and dsRBM2 are close to the pentaloop and the editing site, respectively), indicating that ADAR2 dsRBMs recognize this RNA substrate by themselves, without the deaminase domain. This finding was not obvious considering that the 71 nt RNA that we used contains 34 base pairs, providing potentially 20 different binding sites for a dsRBM, since each dsRBM binds across 15 base pairs (Ramos et al., 2000; Stefl et al., 2005a; Wu et al., 2004). This specific binding apparently originates from dsRBM2, which prefers an RNA duplex containing mismatches over a regular A-form duplex or a stem-loop, and from dsRBM1, which prefers a stem-loop over a regular duplex. The binding preference of ADAR2 dsRBM1 for a stem-loop containing a stable GCU(A/C)A pentaloop is reminiscent of Rnt1p dsRBM structure-specific recognition of the AGNN tetraloop (Wu et al., 2004) and to Staufen dsRBM3 bound to a stem-loop capped by a UUCG tetraloop (Ramos et al., 2000). Interestingly, all three dsRBMs have similar structures, especially regarding the position of α helix 1. This suggests that dsRBMs' binding preference for stem-loop over regular RNA duplexes might be more general than previously expected. In contrast, dsRBM2 favors RNA duplex substrates that contain mismatches and, more particularly, two cytosines involved in A-C mismatches. Although we cannot tell if this recognition is base specific or structure specific (the backbone deformation around the A-C mismatch), to our knowledge, this is the first structural indication that some dsRBMs specifically recognize RNA mismatches.

Scanning force microscopy also revealed that ADAR2 preferentially binds to the R/G stem-loop over regular duplex regions on an RNA mutant substrate in which the R/G stem-loop was inserted into a potato tuber viroid RNA (Klaue et al., 2003). Interestingly, when the duplex irregularities in the R/G stem-loop were mutated to form a more regular duplex, the ADAR2 was still localized in the vicinity of stem-loop structures, including the R/G stem-loop, but not exclusively. This further demonstrates a preference of ADAR2 for stem-loops that would originate from the presence of dsRBM1. Our findings are further supported by a recent biochemical study of ADAR2 in complex with the GluR-B Q/R site with hydroxyl radical cleavage, in which specific RNA binding of the dsRBMs was observed as well (Stephens et al., 2004).

Deletion of dsRBM1 from ADAR2 decreased the editing of the R/G site by 3-fold, and deletion of dsRBM2 decreased the editing of the R/G site by 10-fold. This highlights the importance of dsRBM2 and its exclusive binding to an RNA helix containing two A-C mismatches separated by ten base pairs adjacent to the R/G site. The weak editing activity of ADAR2 that lacks dsRBM2 could be explained by the dual ability of dsRBM1 for binding to both the stem-loop and the A-C mismatch regions of the R/G stem-loop. It suggests that, in certain circumstances, dsRBM1 can replace dsRBM2 in ADAR2 editing. The essential role of the dsRBM2 interaction with A-C mismatches is consistent with several biochemical experiments showing that ADAR2 forms multiple nonspecific complexes when bound to the R/G stem-loop lacking mismatches (Ohman et al., 2000), resulting in a dramatically reduced editing efficiency and selectivity at the R/G site (Kallman et al., 2003). The binding of dsRBM1 to the stem-loop region that contains the structured GCUCA pentaloop is also important, as the variations in the loop sequence and size have an effect on editing efficiency. This interaction is likely to contribute to the overall binding affinity (Macbeth et al., 2004). In conclusion, this structural study suggests that the dsRBMs of ADAR2 appear to preferentially recognize certain structural elements (the stem-loop and the mismatches) of the R/G stem-loop rather than its sequence, explaining why the secondary structure of the R/G stem-loop is very well conserved (Aruscavage and Bass, 2000).

Implication for ADAR Editing

Our structural study of the ADAR2 dsRBMs demonstrates that dsRBMs can specifically recognize certain secondary structure elements of the R/G stem-loop, a natural ADAR2 substrate encoding the B subunit of the AMPA-subtype of glutamate receptor. These

observations indicate that the R/G stem-loop recognition by the ADAR2 dsRBMs is an important determinant for directing the enzyme to the R/G editing site. How is this related to other editing sites? Recent bioinformatics analyses have predicted more than 12,000 new A-to-I editing sites, located predominantly in ALU repetitive elements in the human transcriptome (Athanasiadis et al., 2004; Blow et al., 2004; Levanon et al., 2004). These analyses showed that A-to-I editing is clearly more frequent at adenosines involved in A-C mismatches than at any other mismatches or base pairs. These findings correlate well with the binding preferences of ADAR2 dsRBM2 observed in our study and suggest that the dsRBM2 of ADAR2 may play a more general role in A-to-I editing site selection than previously expected. Of course, not all A-C mismatches are edited by ADAR2, indicating that dsRBM2 is not the only determinant for the specificity of A-to-I conversion. Our data showed that the dsRBM1 prefers to bind irregular RNA elements like stem-loops or non-Watson-Crick base pairs over regular RNA duplexes (in contrast to the dsRBM2 that binds mismatches but not loop regions). The dsRBM1 of ADAR2 may serve to anchor the protein on long, irregular RNA, consistent with the observation that most A-to-I editing sites are embedded within irregular RNA duplexes. ADAR2 dsRBM1 also prevents ADAR2 from editing small RNA duplexes, as suggested by a recent report describing an autoinhibitory role for dsRBM1 (Macbeth et al., 2004).

Experimental Procedures

Plasmids

Plasmids are described in the Supplemental Data.

Tissue Culture and In Vitro Editing Analysis

Human embryonic kidney (HEK293) cells were transiently cotransfected by calcium phosphate precipitation with cDNAs encoding either a control eGFP expression vector (pEGFP-C1; Clontech), eGFP-ADAR2, eGFP-ΔdsRBM1, or eGFP-ΔdsRBM2 in the presence of a 116 bp GluR-B minigene containing the R/G editing site. Crude nuclear extracts (Schreiber et al., 1989) were prepared from HEK293 cells expressing wild-type or mutant eGFP-ADAR2 and were diluted with dialysis buffer to maintain the enzymatic activity (30 mM HEPES [pH 7.6], 300 mM NaCl, 10% glycerol, 1 mM EDTA, 0.5 mM EGTA, 1 mM DTT, 1 mM PMSF, 2 μg/ml Leupeptin, 0.1% Aprotinin) prior to quantitative Western blotting analysis. Mutant proteins were diluted to achieve the same concentration as wild-type eGFP-ADAR2 protein and were incubated with 100 fmol R/G substrate for 30 min at 30ºC. The eGFP-K(127,281)A double mutant was prepared as previously described (Sansam et al., 2003).

In Vitro Editing of R/G Mutants

In vitro editing of R/G mutants is described in the Supplemental Data.

Recombinant Protein Expression and Purification

Several ADAR2 truncations were expressed and purified as previously described (Stefl et al., 2005b).

RNA Preparation

RNA preparation is described in the Supplemental Data.

NMR Spectroscopy

All of the NMR experiments were conducted at 293 K (or at 315 K) on Bruker Avance-900 and DRX-750, 600, and 500 MHz spectrometers. A detailed description of the resonance assignment procedure of the studied proteins is given elsewhere (Stefl et al., 2005b). RNAs were assigned mostly based on NOESY data, since through-bond techniques suffer from the loss of signal in large RNAs. Specifically, a 2D homonuclear NOESY and TOCSY measured on unlabeled R/G stem-loop RNA, 2D-filtered/edited NOESY experiments (Peterson et al., 2004), a 3D [^{1}H,^{13}C,^{1}H]-NOESY acquired on four base type-specific ^{13}C,^{15}N-(A)-,^{13}C,^{15}N-(U)-,^{13}C^{15}N-(G)-,^{13}C^{15}N-(C)-labeled R/G stem-loop RNAs, and the use of the resonance assignments of the subfragments (Figure 1) were essential in achieving sequential assignment. A full list of experiments used for free and bound proteins and RNAs is given in Table S1. All spectra were processed with XWINNMR (Bruker) and were analyzed with Sparky (Goddard and Kneller, 2004).

Structure Calculations

The preliminary structure determination was performed with the automated NOE assignment module CANDID (Herrmann et al., 2002) in the DYANA program (Guntert et al., 1997). CANDID/DYANA carries out automated assignment and distance calibration of NOE intensities, removal of meaningless restraints, structure calculation with torsion angle dynamics, and automatic upper distance limit violation analysis. The resultant NOE crosspeak assignments were subsequently confirmed by visual inspection of the spectra. In the next step, CANDID/DYANA-generated restraints were used for further refinement of the preliminary structures with AMBER 7.0 software (Case et al., 2002); this process employed a force field described by Cornell et al. (1995), a refinement protocol described in Padrta et al. (2002), and the generalized-Born solvation model (Bashford and Case, 2000). Molecular graphics were generated by using PyMOL (DeLano, 2002) and NUCCYL (Jovine, 2003).

Model for RNA Binding

The model for RNA binding is described in the Supplemental Data.

Use of Sequence/Structure Databases and Sequence Alignments

Sequence/structure databases and sequence alignments are described in the Supplemental Data.

Light-Scattering Experiments

Light-scattering experiments are described in the Supplemental Data.

Supplemental Data

Supplemental Data including Figures S1–S4 are available at http://www.structure.org/cgi/content/full/14/2/345/DC1/.

Acknowledgments

We thank Dr. E. Zobeley for assistance with the light-scattering instrument and Drs. J. D. Alfonso and M.-A. Rubio for insightful discussions. We are grateful to Prof. G. Wagner for the gift of the pET30-GB*Fusion*1 vector. The authors are supported by the Swiss National Science Foundation (Nr. 3100A0-107713), the Roche Research Fund for Biology at the Eidgenössisch Technische Hochschule Zurich (F.H.-T.A.), the National Institutes of Health (RBE; NS33323), and the European Molecular Biology Organization and the Human Frontier Science Program postdoctoral fellowships (R.S.). F.H.T.A. is a European Molecular Biology Organization Young Investigator.

Received: May 6, 2005
Revised: October 26, 2005
Accepted: November 1, 2005
Published: February 10, 2006

References

Allain, F.H., Bouvet, P., Dieckmann, T., and Feigon, J. (2000). Molecular basis of sequence-specific recognition of pre-ribosomal RNA by nucleolin. EMBO J. *19*, 6870–6881.

Aruscavage, P.J., and Bass, B.L. (2000). A phylogenetic analysis reveals an unusual sequence conservation within introns involved in RNA editing. RNA *6*, 257–269.

Athanasiadis, A., Rich, A., and Maas, S. (2004). Widespread A-to-I RNA editing of Alu-containing mRNAs in the human transcriptome. PLoS Biol. *2*, e391.

Bashford, D., and Case, D.A. (2000). Generalized born models of macromolecular solvation effects. Annu. Rev. Phys. Chem. *51*, 129–152.

Bass, B.L. (2002). RNA editing by adenosine deaminases that act on RNA. Annu. Rev. Biochem. *71*, 817–846.

Bass, B.L., and Weintraub, H. (1988). An unwinding activity that covalently modifies its double-stranded RNA substrate. Cell *55*, 1089–1098.

Bhalla, T., Rosenthal, J.J., Holmgren, M., and Reenan, R. (2004). Control of human potassium channel inactivation by editing of a small mRNA hairpin. Nat. Struct. Mol. Biol. *11*, 950–956.

Blaszczyk, J., Gan, J., Tropea, J.E., Court, D.L., Waugh, D.S., and Ji, X. (2004). Noncatalytic assembly of ribonuclease III with double-stranded RNA. Structure (Camb) *12*, 457–466.

Blow, M., Futreal, P.A., Wooster, R., and Stratton, M.R. (2004). A survey of RNA editing in human brain. Genome Res. *14*, 2379–2387.

Burns, C.M., Chu, H., Rueter, S.M., Hutchinson, L.K., Canton, H., Sanders-Bush, E., and Emeson, R.B. (1997). Regulation of serotonin-2C receptor G-protein coupling by RNA editing. Nature *387*, 303–308.

Bycroft, M., Grunert, S., Murzin, A.G., Proctor, M., and Stjohnston, D. (1995). Nmr solution structure of a Dsrna binding domain from *Drosophila* Staufen protein reveals homology to the N-terminal domain of ribosomal-protein S5. EMBO J. *14*, 3563–3571.

Carlson, C.B., Stephens, O.M., and Beal, P.A. (2003). Recognition of double-stranded RNA by proteins and small molecules. Biopolymers *70*, 86–102.

Case, D.A., Pearlman, D.A., Caldwell, J.W., Cheatham, T.E., III, Wang, J., Ross, W.S., Simmerling, C.L., Darden, T.A., Merz, K.M., Stanton, R.V., et al. (2002). AMBER 7 (http://amber.scripps.edu/).

Cho, D.S., Yang, W., Lee, J.T., Shiekhattar, R., Murray, J.M., and Nishikura, K. (2003). Requirement of dimerization for RNA editing activity of adenosine deaminases acting on RNA. J. Biol. Chem. *278*, 17093–17102.

Cornell, W.D., Cieplak, P., Bayly, C.I., Gould, I.R., Merz, K.M., Ferguson, D.M., Spellmeyer, D.C., Fox, T., Caldwell, J.W., and Kollman, P.A. (1995). A 2nd generation force-field for the simulation of proteins, nucleic-acids, and organic-molecules. J. Am. Chem. Soc. *117*, 5179–5197.

Dawson, T.R., Sansam, C.L., and Emeson, R.B. (2004). Structure and sequence determinants required for the RNA editing of ADAR2 substrates. J. Biol. Chem. *279*, 4941–4951.

DeLano, W.L. (2002). The PyMOL Molecular Graphics System (http://www.pymol.org).

Deo, R.C., Bonanno, J.B., Sonenberg, N., and Burley, S.K. (1999). Recognition of polyadenylate RNA by the poly(A)-binding protein. Cell *98*, 835–845.

Dominguez, C., Boelens, R., and Bonvin, A.M. (2003). HADDOCK: a protein-protein docking approach based on biochemical or biophysical information. J. Am. Chem. Soc. *125*, 1731–1737.

Doyle, M., and Jantsch, M.F. (2002). New and old roles of the double-stranded RNA-binding domain. J. Struct. Biol. *140*, 147–153.

Egebjerg, J., and Heinemann, S.F. (1993). Ca^{2+} permeability of unedited and edited versions of the kainate selective glutamate receptor GluR6. Proc. Natl. Acad. Sci. USA *90*, 755–759.

Emeson, R.B., and Singh, M. (2000). Adenosine to inosine RNA editing: substrates and consequences. In RNA Editing: Frontiers in Molecular Biology, B.L. Bass, ed. (London: Oxford University Press), pp. 109–138.

Fierro-Monti, I., and Mathews, M.B. (2000). Proteins binding to duplexed RNA: one motif, multiple functions. Trends Biochem. Sci. *25*, 241–246.

Gallo, A., Keegan, L.P., Ring, G.M., and O'Connell, M.A. (2003). An ADAR that edits transcripts encoding ion channel subunits functions as a dimer. EMBO J. *22*, 3421–3430.

Gerber, A.P., and Keller, W. (2001). RNA editing by base deamination: more enzymes, more targets, new mysteries. Trends Biochem. Sci. *26*, 376–384.

Goddard, T.D., and Kneller, D.G. (2004). SPARKY 3 (http://www.cgl.ucsf.edu/home/sparky).

Guntert, P., Mumenthaler, C., and Wuthrich, K. (1997). Torsion angle dynamics for NMR structure calculation with the new program DYANA. J. Mol. Biol. *273*, 283–298.

Handa, N., Nureki, O., Kurimoto, K., Kim, I., Sakamoto, H., Shimura, Y., Muto, Y., and Yokoyama, S. (1999). Structural basis for recognition of the tra mRNA precursor by the Sex-lethal protein. Nature *398*, 579–585.

Herrmann, T., Guntert, P., and Wuthrich, K. (2002). Protein NMR structure determination with automated NOE assignment using the new software CANDID and the torsion angle dynamics algorithm DYANA. J. Mol. Biol. *319*, 209–227.

Hoopengardner, B., Bhalla, T., Staber, C., and Reenan, R. (2003). Nervous system targets of RNA editing identified by comparative genomics. Science *301*, 832–836.

Jaikaran, D.C., Collins, C.H., and MacMillan, A.M. (2002). Adenosine to inosine editing by ADAR2 requires formation of a ternary complex on the GluR-B R/G site. J. Biol. Chem. *277*, 37624–37629.

Jovine, L. (2003). NUCCYL (http://www.biosci.ki.se/groups/ljo/software/nuccyl.html).

Kallman, A.M., Sahlin, M., and Ohman, M. (2003). ADAR2 A→I editing: site selectivity and editing efficiency are separate events. Nucleic Acids Res. *31*, 4874–4881.

Keegan, L.P., Gallo, A., and O'Connell, M.A. (2001). The many roles of an RNA editor. Nat. Rev. Genet. *2*, 869–878.

Kharrat, A., Macias, M.J., Gibson, T.J., Nilges, M., and Pastore, A. (1995). Structure of the Dsrna binding domain of *Escherichia coli* Rnase-Iii. EMBO J. *14*, 3572–3584.

Klaue, Y., Kallman, A.M., Bonin, M., Nellen, W., and Ohman, M. (2003). Biochemical analysis and scanning force microscopy reveal productive and nonproductive ADAR2 binding to RNA substrates. RNA *9*, 839–846.

Kohler, M., Burnashev, N., Sakmann, B., and Seeburg, P.H. (1993). Determinants of Ca^{2+} permeability in both TM1 and TM2 of high affinity kainate receptor channels: diversity by RNA editing. Neuron *10*, 491–500.

Laskowski, R.A., Rullmannn, J.A., MacArthur, M.W., Kaptein, R., and Thornton, J.M. (1996). AQUA and PROCHECK-NMR: programs for checking the quality of protein structures solved by NMR. J. Biomol. NMR *8*, 477–486.

Leulliot, N., Quevillon-Cheruel, S., Graille, M., Van Tilbeurgh, H., Leeper, T.C., Godin, K.S., Edwards, T.E., Sigurdsson, S.T., Rozenkrants, N., Nagel, R.J., et al. (2004). A new α-helical extension promotes RNA binding by the dsRBD of Rnt1p RNAse III. EMBO J. *23*, 2468–2477.

Levanon, E.Y., Eisenberg, E., Yelin, R., Nemzer, S., Hallegger, M., Shemesh, R., Fligelman, Z.Y., Shoshan, A., Pollock, S.R., Sztybel, D., et al. (2004). Systematic identification of abundant A-to-I editing sites in the human transcriptome. Nat. Biotechnol. *22*, 1001–1005.

Lomeli, H., Mosbacher, J., Melcher, T., Hoger, T., Geiger, J.R., Kuner, T., Monyer, H., Higuchi, M., Bach, A., and Seeburg, P.H. (1994). Control of kinetic properties of AMPA receptor channels by nuclear RNA editing. Science *266*, 1709–1713.

Lu, D., Searles, M.A., and Klug, A. (2003). Crystal structure of a zinc-finger-RNA complex reveals two modes of molecular recognition. Nature *426*, 96–100.

Macbeth, M.R., Lingam, A.T., and Bass, B.L. (2004). Evidence for auto-inhibition by the N terminus of hADAR2 and activation by dsRNA binding. RNA *10*, 1563–1571.

Macbeth, M.R., Schubert, H.L., Vandemark, A.P., Lingam, A.T., Hill, C.P., and Bass, B.L. (2005). Inositol hexakisphosphate is bound in the ADAR2 core and required for RNA editing. Science *309*, 1534–1539.

Morse, D.P., and Bass, B.L. (1999). Long RNA hairpins that contain inosine are present in *Caenorhabditis elegans* poly(A)+ RNA. Proc. Natl. Acad. Sci. USA *96*, 6048–6053.

Morse, D.P., Aruscavage, P.J., and Bass, B.L. (2002). RNA hairpins in noncoding regions of human brain and Caenorhabditis elegans mRNA are edited by adenosine deaminases that act on RNA. Proc. Natl. Acad. Sci. USA *99*, 7906–7911.

Mulder, F.A., Schipper, D., Bott, R., and Boelens, R. (1999). Altered flexibility in the substrate-binding site of related native and engineered high-alkaline *Bacillus subtilisins*. J. Mol. Biol. *292*, 111–123.

Nanduri, S., Carpick, B.W., Yang, Y.W., Williams, B.R.G., and Qin, J. (1998). Structure of the double-stranded RNA-binding domain of the protein kinase PKR reveals the molecular basis of its dsRNA-mediated activation. EMBO J. *17*, 5458–5465.

Ohman, M., Kallman, A.M., and Bass, B.L. (2000). In vitro analysis of the binding of ADAR2 to the pre-mRNA encoding the GluR-B R/G site. RNA *6*, 687–697.

Padrta, P., Stefl, R., Kralik, L., Zidek, L., and Sklenar, V. (2002). Refinement of d(GCGAAGC) hairpin structure using one- and two-bond residual dipolar couplings. J. Biomol. NMR *24*, 1–14.

Peterson, R.D., Theimer, C.A., Wu, H., and Feigon, J. (2004). New applications of 2D filtered/edited NOESY for assignment and structure elucidation of RNA and RNA-protein complexes. J. Biomol. NMR *28*, 59–67.

Ramos, A., Grunert, S., Adams, J., Micklem, D.R., Proctor, M.R., Freund, S., Bycroft, M., St Johnston, D., and Varani, G. (2000). RNA recognition by a Staufen double-stranded RNA-binding domain. EMBO J. *19*, 997–1009.

Rueter, S.M., Dawson, T.R., and Emeson, R.B. (1999). Regulation of alternative splicing by RNA editing. Nature *399*, 75–80.

Ryter, J.M., and Schultz, S.C. (1998). Molecular basis of double-stranded RNA-protein interactions: structure of a dsRNA-binding domain complexed with dsRNA. EMBO J. *17*, 7505–7513.

Sansam, C.L., Wells, K.S., and Emeson, R.B. (2003). Modulation of RNA editing by functional nucleolar sequestration of ADAR2. Proc. Natl. Acad. Sci. USA *100*, 14018–14023.

Schreiber, E., Matthias, P., Muller, M.M., and Schaffner, W. (1989). Rapid detection of octamer binding proteins with 'mini-extracts,' prepared from a small number of cells. Nucleic Acids Res. *17*, 6419.

Seeburg, P.H., Higuchi, M., and Sprengel, R. (1998). RNA editing of brain glutamate receptor channels: mechanism and physiology. Brain Res. Brain Res. Rev. *26*, 217–229.

Sommer, B., Kohler, M., Sprengel, R., and Seeburg, P.H. (1991). RNA editing in brain controls a determinant of ion flow in glutamate-gated channels. Cell *67*, 11–19.

Stefl, R., and Allain, F.H. (2005). A novel RNA pentaloop fold involved in targeting ADAR2. RNA *11*, 592–597.

Stefl, R., Skrisovska, L., and Allain, F.H. (2005a). RNA sequence- and shape-dependent recognition by proteins in the ribonucleoprotein particle. EMBO Rep. *6*, 33–38.

Stefl, R., Skrisovska, L., Xu, M., Emeson, R.B., and Allain, F.H. (2005b). Resonance assignments of the double-stranded RNA-binding domains of adenosine deaminase acting on RNA 2 (ADAR2). J. Biomol. NMR *31*, 71–72.

Stephens, O.M., Haudenschild, B.L., and Beal, P.A. (2004). The binding selectivity of ADAR2's dsRBMs contributes to RNA-editing selectivity. Chem. Biol. *11*, 1239–1250.

Tonkin, L.A., and Bass, B.L. (2003). Mutations in RNAi rescue aberrant chemotaxis of ADAR mutants. Science *302*, 1725.

Wong, T.C., Ayata, M., Ueda, S., and Hirano, A. (1991). Role of biased hypermutation in evolution of subacute sclerosing panencephalitis virus from progenitor acute measles virus. J. Virol. *65*, 2191–2199.

Wu, H., Henras, A., Chanfreau, G., and Feigon, J. (2004). Structural basis for recognition of the AGNN tetraloop RNA fold by the double-stranded RNA-binding domain of Rnt1p RNase III. Proc. Natl. Acad. Sci. USA *101*, 8307–8312.

Zhang, Z., and Carmichael, G.G. (2001). The fate of dsRNA in the nucleus: a p54(nrb)-containing complex mediates the nuclear retention of promiscuously A-to-I edited RNAs. Cell *106*, 465–475.

Zhou, P., Lugovskoy, A.A., and Wagner, G. (2001). A solubility-enhancement tag (SET) for NMR studies of poorly behaving proteins. J. Biomol. NMR *20*, 11–14.

Accession Numbers

Coordinates have been deposited into the Protein Data Bank with accession codes 2B7T and 2B7V for dsRBM1 and dsRBM2, respectively.